Anti-cross-correlation between the adjacent open and closed durations of Markovian channels

Yandong Huang,[1] Jing Qu,[2] Xiang Li,[2] Fang Wei,[2] Jinjin Zhong,[2] Yuning Wu,[2] Meichun Cai,[2] Xuejuan Gao,[2] John E. Pearson,[3] and Jianwei Shuai[2,4,5,*]

[1]*College of Computer Engineering, Jimei University, Xiamen 361021, China*
[2]*Department of Physics, Xiamen University, Xiamen 361005, China*
[3]*Theoretical Biology and Biophysics, Los Alamos National Laboratory, Los Alamos, New Mexico 87545, USA*
[4]*State Key Laboratory of Cellular Stress Biology, Innovation Center for Cell Signaling Network, Xiamen University, Xiamen 361102, China*
[5]*National Institute for Data Science in Health and Medicine, Xiamen University, Xiamen 361102, China*

(Received 1 March 2019; revised manuscript received 14 January 2020; published 31 January 2020)

We show that a non-Markovian behavior can appear in a type of Markovian multimeric channel. Such a channel consists of N independent subunits, and each subunit has at least one open state and more than one closed state. Suppose the open state of the channel is defined as M out of N subunits in the open state with $N > M > 0$. We show that, although the gating dynamics for each subunit between open and closed states is Markovian, the channel can show a memory behavior of weak anti-cross-correlation between the adjacent open and closed durations. Our study indicates that a non-Markovian binary time series can be obtained from a linear superposition of some independent channel subunits with Markovian gating dynamics.

DOI: 10.1103/PhysRevE.101.012418

I. INTRODUCTION

Ion channels, which transport various ions into or out of biological membranes, play important roles in many physiological processes, such as secretion, regulation, memory, and signal transduction. With the patch clamp technique, one can record single-channel ion currents with a time resolution of 1 ms [1]. The small background and large currents measured by the patch clamp actually correspond to the closed and open states of the channel, respectively. The analysis of the ion current can then reveal the stochastic gating dynamics of the ion channels. At the first stage, one can simply assume that the stochastic behavior of the channel gating is Markovian. Therefore, the recorded current data are modeled with the assumption that the channel kinetics is a Markovian process stochastically jumping among a small number of discrete states [2,3].

However, clear evidence also shows that the stochastically open and closed dynamics of some channels are non-Markovian [4–6]. Different non-Markovian behaviors have been discussed, including long-range correlation, $1/f$ noise, long-term persistent or antipersistent process, and anti-cross-correlation. The non-Markovian channel currents can be generated with the equilibrium gating dynamics among multiple open and closed states with multiple transition pathways [5,6]. A statistical test is presented to determine whether stochastic data obtained from channel currents are Markovian or non-Markovian [7]. For the large conductance locust potassium (BK) channel, a long-range correlation is observed for the closed states [8]. The non-Markovian data can also be directly produced in a channel model with the nonequilibrium time-dependent gating dynamics among the channel states [9].

The stochastic channel current can present long time memory effect as the $1/f$ noise [10–16]. The $1/f$ noise can be caused by the equilibrium conductance fluctuations related to the conformational flexibility of the structural geometry of channel pores [10,11]. It was shown that the low-frequency $1/f$ noise in fabricated solid-state nanopores is related to the number of charge carriers, as described by the Hooge relation [12]. The long time memory can also be studied by the Hurst exponent or self-similarity parameter H with rescaled range analysis, detrended fluctuation analysis, or the periodogram regression method [17–19]. A Hurst exponent of $H = 0.5$ is typically observed with white noise, while a long-term persistent process induces $H > 0.5$ and an antipersistent time series leads to $H < 0.5$.

Besides the long time memory, non-Markovian correlation can also occur at short timescale. It has been shown that, for Ca^{2+} puffs which are released from a cluster of inositol 1,4,5-trisphosphate receptors (IP_3Rs), the interpuff intervals tend to be longer after large puffs and tend to be shorter after small puffs, giving a positive correlation between puff amplitude and interpuff interval [20]. However, the simulation results indicate that the correlation between successive puff amplitudes can be negative [21]. For sparks which are released from a cluster of ryanodine receptors (RyRs), the correlation between spark amplitude and spark rising time can also be negative [22]. Thus the negative correlation displays a behavior of the anti-cross-correlation (ACC) at the clustered channel level. Biologically, these different correlation relationships reveal different underlying microscopic kinetics of channels, including the termination mechanism or stochastic attrition [21,22].

We show in the paper that a non-Markovian behavior of ACC can be generated at the single-channel level with a class

*Present address: Department of Physics, Xiamen University, Xiamen 361005, China; jianweishuai@xmu.edu.cn

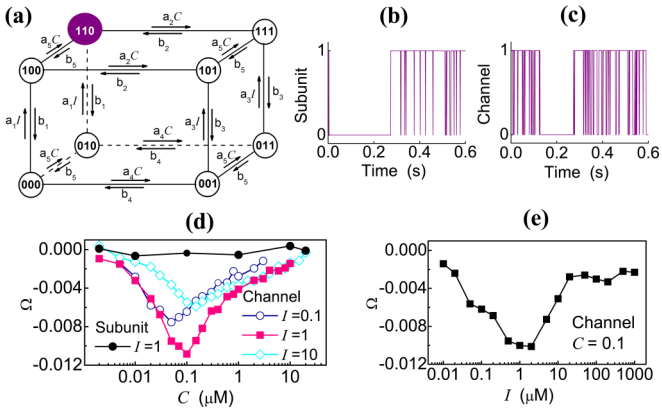

FIG. 1. The De Young–Keizer model. (a) The eight-state IP_3R subunit model. (b) The stochastically gating dynamics between the open and closed states for a subunit, and (c) the stochastic dynamics between the open and closed states for the channel at $I = 10$ and $C = 0.1\ \mu M$. (d) The cross correlation Ω as a function of C, in which the solid black cycles are for a single IP_3R subunit at $I = 1\ \mu M$, and the open navy circles, solid pink squares, and open cyan diamonds are for IP_3R channel at $I = 0.1$, 1, and 10 μM, respectively. (e) The cross correlation Ω for the channel as a function of I. The model parameters are $K_4 = K_1K_2/K_3$, $K_1 = 0.13$, $K_2 = 1.05$, $K_3 = 0.94$, $K_5 = 0.08$ mM, $a_1 = 400$, $a_2 = 0.2$, $a_3 = 400$, $a_4 = 0.2$, and $a_5 = 20\ \mu M^{-1}\ s^{-1}$ with $b_i = a_iK_i$ as given in [27].

of Markovian channels. Many ion channels are comprised of several independent subunits. Suppose that a channel consists of N identical and independent subunits, and each subunit has more than one closed state and at least one open state. The open state of the channel is defined as at least M out of N subunits are in the open state with $N > M > 0$. Then the correlation between the adjacent open and closed durations of the channel displays a weak ACC behavior, even though each subunit has Markovian gating dynamics.

II. ACC IN STOCHASTIC IP_3R CHANNEL MODELS

As an example we first discuss the stochastically open and closed dynamics of the tetrameric IP_3R channels [23]. The IP_3Rs are intracellular Ca^{2+} channels that are regulated by Ca^{2+} and IP_3. It was found that IP_3Rs are distributed at the single-channel state on plasma membrane [24] or at the clustered channel state on the endoplasma membrane [25]. Different models have been suggested to simulate the IP_3R dynamics [26–34]. An IP_3R model [27] was proposed by De Young and Keizer to describe the patch clamp data obtained from IP_3R reconstituted in a bilayer membrane *in vitro* [28]. A modified De Young–Keizer IP_3R model comprises four identical and independent subunits [29]. In each subunit, there are three independent binding sites, i.e., an activating Ca^{2+}-binding site, an inhibitory Ca^{2+}-binding site, and an IP_3-binding site. Thus, there are eight states for a subunit which can be described by (ijk) with the indexes i, j, and k representing the occupied (=1) or nonoccupied (=0) state at IP_3, activating Ca^{2+}, and inhibitory Ca^{2+}-binding site, respectively. A schematic picture of the transitions among these eight states of the subunit is shown in Fig. 1(a). The (110) state bound with an IP_3 and an activating Ca^{2+} is called the open state, and the others are closed states. The channel is open when three or four subunits are in the open state [29].

In the paper we focus on the stochastic channel dynamics at constant Ca^{2+} concentration C and IP_3 concentration I, which corresponds to the patch clamp experiments [35]. To simulate the Markovian dynamics of subunits, the transition probability in the simulation is defined by $k\delta t$ for a transition process with transition rate k in a small time step δt. Random numbers homogeneously distributed in [0,1] are generated at each time step and compared with transition probabilities to determine to which state each subunit will transfer [36]. As a consequence, the detailed states for all the subunits of the channel can be traced and updated at every time step. Accordingly, both the stochastic durations of open and closed states for each subunit [Fig. 1(b)] and the stochastic durations of open and closed states of the channel [Fig. 1(c)] can be obtained.

Then we calculate the cross correlations between the adjacent active and resting time durations of individual subunits and between the adjacent open and closed durations of the channel. The cross correlation Ω between two time series $\{t_o\}$ and $\{t_c\}$ is defined as

$$\Omega = \frac{\langle(\langle t_o\rangle - t_o)(\langle t_c\rangle - t_c)\rangle}{\sqrt{\langle(\langle t_o\rangle - t_o)^2\rangle}\sqrt{\langle(\langle t_c\rangle - t_c)^2\rangle}} = \frac{\langle t_o t_c\rangle - \langle t_o\rangle\langle t_c\rangle}{\sqrt{\langle t_o^2\rangle - \langle t_o\rangle^2}\sqrt{\langle t_c^2\rangle - \langle t_c\rangle^2}}, \quad (1)$$

where $\langle\cdots\rangle$ represents the averaging process.

As expected, the cross correlation for each subunit is around zero [solid black cycles in Fig. 1(d)]. Intriguingly, the cross-correlation is typically negative for the channel as a function of C at different I [Fig. 1(d)]. Although each subunit has a zero cross correlation between the adjacent open and closed durations, the channel which consists of four independent subunits shows a weak ACC between the adjacent open and closed durations. Such a negative correlation means that a short (or long) open time duration for the channel is more likely to be followed by a long (or short) closed time duration and vice versa. Figure 1(e) shows that an ACC can also be found for the channel between the open and closed durations as a function of I at $C = 0.1\ \mu M$.

Another modified IP_3R model [37] has been proposed to describe patch clamp data recorded from IP_3R in the native environment of the nuclear envelope in the *Xenopus* oocyte [35]. Compared to the original De Young–Keizer model, the new model further includes a conformational change [37], whereby a subunit in the (110) state (i.e., only with one IP_3 and one activating Ca^{2+} bound) is "inactive," and it must change through a conformational transition to the open state (A) before it can contribute to the channel open state. The model also assumes that the channel is open when either three or four subunits are in the open state. A schematic diagram of the state transitions for a subunit is shown in Fig. 2(a).

For this model, each subunit has a constant mean time $t = 1/b_0$ in the open state, which is independent of C or I. The zero correlation between the adjacent open and closed durations at $I = 10\ \mu M$ for a single subunit is given as a function C in Fig. 2(b) with solid cycles. As a comparison,

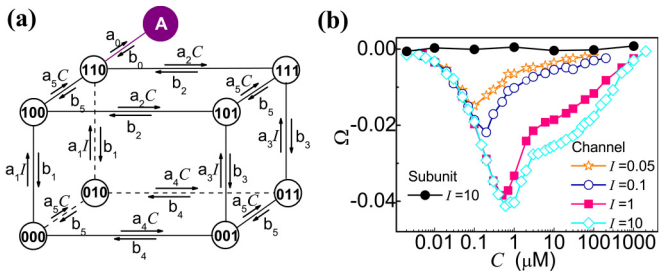

FIG. 2. The modified De Young–Keizer model with allosteric activation. (a) The nine-state structure of IP_3R subunit. The parameters are reaction dissociation constants ($K_1 = 0.0036$, $K_2 = 16$, $K_3 = 0.8$, $K_5 = 0.8\ \mu M$, and $K_4 = K_1K_2/K_3$) and binding rates ($a_1 = 60$, $a_2 = 0.2$, $a_3 = 5$, $a_4 = 0.5$, $a_5 = 150\ \mu M^{-1}\,s^{-1}$) with unbinding rates $b_i = a_iK_i$ as given in [37]. Related to the open state A, $a_0 = 540\ \mu M^{-1}\,s^{-1}$ and $b_0 = 80\ s^{-1}$ (b) For stochastic IP_3R channel, Ω via C are plotted at $I = 0.05$ (open orange star), 0.1 (open navy circle), 1 (solid pink square), and 10 μM (open cyan diamond). For a single IP_3R subunit, Ω via C at $I = 10\ \mu M$ is given with solid black circles.

the cross correlations between the adjacent open and closed durations of the channel are plotted in Fig. 2(b) as a function of C at $I = 0.01$, 0.1, and 1 μM, respectively. Again, a weak ACC for channel dynamics is observed in the model.

For the tetrameric IP_3R channel, one can assume that the channel is open when all of the four subunits are in the open state where the subunit can be either the eight-state [Fig. 1(a)] or the nine-state model [Fig. 2(a)]. However, with such a model, one cannot observe any correlation relationship between the adjacent open and closed durations of the channel (data not shown).

III. GENERATOR MATRIX THEORY FOR CHANNEL DYNAMICS

In this section we first introduce the generator matrix theory to discuss the channel dynamics [38]. Generally the open probability P_O, the mean open time τ_O, and closed time τ_C of a channel can be given by

$$\tau_O = \frac{P_O}{J}, \quad \tau_C = \frac{P_C}{J}, \tag{2}$$

where $P_C = 1 - P_O$ is the closed probability and J the equilibrium probability flux from open states to closed states. We can write P_O in terms of un-normalized open and closed probabilities P_{Oi} and P_{Ci} for all the open and closed states, which are relative to a reference state given by unity probability. Normally taking the reference state to be an unliganded closed state, i.e., $P_{C0} = 1$, we have

$$P_O = \frac{\sum_i p_{Oi}}{Z}, \quad P_C = \frac{\sum_i p_{Ci}}{Z}, \tag{3}$$

where $Z = \sum_i p_{Oi} + \sum_i p_{Ci}$ is the normalized factor, so that $P_O + P_C = 1$.

The probability flux J is given by

$$J = \frac{\sum_i k_i^{OC} p_{Oi}}{z}, \tag{4}$$

where k_i^{OC} is the transition rate from the open to closed state out of the ith open state. In terms of the transition matrix Q_{OC} from the open to closed state and the vector of open probabilities w_O, the probability flux from the open to closed state can be written as

$$J = w_O Q_{OC} u_O, \tag{5}$$

where u_O is a vector of N_O ones, if there are N_O open states.

At the equilibrium state all fluxes balance, so that the flux from the closed to open state equals the flux from the open to closed state, i.e., $w_O Q_{OC} u_O = w_C Q_{CO} u_C$, where w_C is the vector of closed probabilities. If there is more than one pathway out of the ith open state into various closed states, then k_i^{OC} is the sum of all such rates. If there is no such pathway, then $k_i^{OC} = 0$. In the simplest case of one open state, τ_O is given by $1/k^{OC}$ and so that, if no pathway out of the open state requires ligand binding, τ_O is a constant.

The agonist-activated ion channels are typically studied by varying ligand concentrations. If the binding kinetics obeys the law of mass action and the detailed balance, the relative probability for an open state with i ligands bound is $K_{Oi}L^i$, where K_{Oi} is the product of the inverse disassociation constants along any path from the unliganded closed reference state to the open state under consideration and L^i is the ligand concentration. If more than one state has i ligands bound, one can still take the relative occupancy of all states with i ligands bound to be $K_{Oi}L^i$ but now K_{Oi} has to be taken as the sum over all states with i ligands bound of the products of the inverse disassociation constants. The open and closed probabilities and the flux can then be written as [39]

$$P_O = \frac{\sum_i K_{Oi}L^i}{Z}, \quad P_C = \frac{\sum_i K_{Ci}L^i}{Z}, \quad J = \frac{\sum_i J_i L^i}{Z}. \tag{6}$$

In this paper we analyze the cross correlation of the model based on the matrix theory. The cross correlation between the adjacent open and closed durations can be given by

$$\Omega = \pi_O Q_{OO}^2 Q_{OC} Q_{CC}^{-2} Q_{CO} u_O, \tag{7}$$

where $\pi_O = w_O Q_{CO}/J$ is the entry probability for the open states with w_O the vector of open probabilities, and Q_{OO}, Q_{OC}, Q_{CO}, and Q_{CC} are the transition rate matrices of open to open state, open to closed state, closed to open state and closed to closed state, respectively.

IV. ACC IN A STOCHASTIC TOY MODEL

Here we apply the generator matrix theory above to discuss a toy channel model. The toy channel has two identical and independent subunits. Each subunit has three states: two closed states (C_1 and C_2) and an open state (O), given as

$$C_1 \underset{k_2}{\overset{k_1}{\rightleftarrows}} C_2 \underset{k_4}{\overset{k_3 L}{\rightleftarrows}} O, \tag{8}$$

where L is the ligand concentration, and constants k_1, k_2, k_3, and k_4 donate the reaction rates. The channel is open when at least one of the two subunits is in the open state. For this model, each subunit has a mean time $\tau_A = 1/(k_4)$ in the open state.

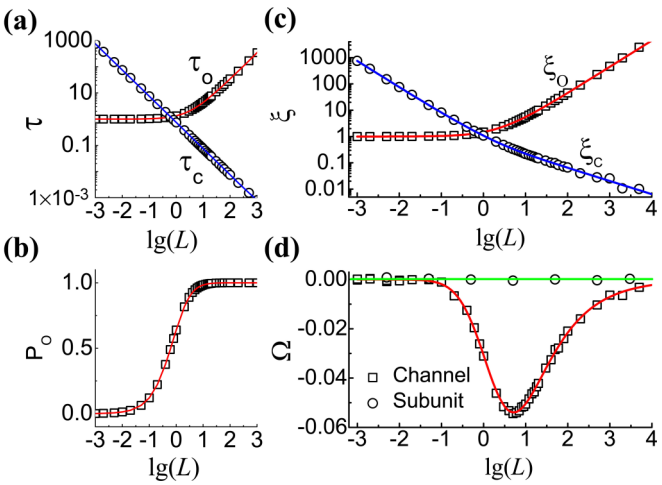

FIG. 3. For the stochastic dimer channel, (a) the mean open time τ_O (squares) and closed time τ_C (circles), (b) the open probability of channel P_O, (c) ξ_O (square) and ξ_C (circle), and (d) Ω (square) against the ligand concentration L with numerical simulation, as well as the theoretical analysis (solid line). For a single subunit, Ω in (d) is plotted with theoretical analysis (green dashed line) and numerical simulation (circle).

For each subunit with only a single open state, the distributions of the open and closed times satisfy

$$f_{OC}(t_O, t_C) = f_O(t_O) f_C(t_C), \tag{9}$$

where $f_O(t_O)$, $f_C(t_C)$, $f_{OC}(t_O, t_C)$ are the distributions of open time t_O, closed time t_C, and time $t_O + t_C$ for the stochastic subunit, respectively. It follows immediately that the covariance is zero and the cross correlation is also identically zero.

Now we consider the properties of the channel defined in Eq. (8). With the matrix theory [38,39], the channel open probability P_O and the probability flux J are given by

$$P_O = w_A^2 + 2w_A(1 - w_A), \quad J = 4k_4 w_A(1 - w_A), \tag{10}$$

where $w_A = k_1 k_3 L/(k_2 k_4 Z)$ is the probability for each subunit in the open state with the normalization factor

$$\mathrm{Z} = 1 + k_1/k_2 + k_1 k_3 L/(k_2 k_4). \tag{11}$$

Then, putting the transition rate matrix into Eq. (7), finally we have

$$\begin{aligned} \Omega &= -\frac{\Gamma_2}{4k_4 ABC}, \\ \langle \tau_O^2 \rangle &= \frac{Ck_4(4k_4 A + 5\Gamma_1) + k_3 L \Gamma_1 D}{2k_4^4 AC}, \\ \langle \tau_C^2 \rangle &= \frac{A^2(A^2 + \Gamma_1 + 2\Gamma_2) + \Gamma_2^2}{2\Gamma_1^2 AB}, \end{aligned} \tag{12}$$

with $\Gamma_1 = k_1 k_3 L$, $\Gamma_2 = k_2 k_3 L$, $A = k_1 + k_2$, $B = k_3 L + A$, $C = k_4 + A$, and $\mathrm{D} = k_1 + k_4$.

As an example, we let $k_1 = 0.2$, $k_2 = 0.1$, $k_3 = k_4 = 1.0$, and vary L. The analytic results for variables τ_O, τ_C, P_O, ξ_O, ξ_C, and Ω against L are given in Figs. 3(a)–3(d) with solid lines, respectively. For such a simple model, although each subunit has an uncorrelated gating kinetics, the channel shows a weak ACC behavior between the adjacent open and closed durations.

One can directly simulate the stochastic dynamics of the toy model also. With the Markovian simulation, the stochastic open and closed states can be obtained for the channel. As a result, one can calculate the mean open time τ_O, mean close time τ_C, and the open probability P_O, as well as the cross correlation Ω as a function of L. The simulation results are given in Figs. 3(a)–3(d) with symbols.

Now we discuss the origination of the ACC in such channel systems. Actually, the two-subunit model has six channel states, given as

$$\begin{array}{ccccc} C_1C_1 & \underset{k_2}{\overset{2k_1}{\rightleftharpoons}} & C_1C_2 & \underset{2k_2}{\overset{k_1}{\rightleftharpoons}} & C_2C_2 \\ & & k_4 \uparrow\downarrow k_3 L & & k_4 \uparrow\downarrow 2k_3 L \\ & & C_1O & \underset{k_2}{\overset{k_1}{\rightleftharpoons}} & C_2O \underset{2k_4}{\overset{k_3 L}{\rightleftharpoons}} OO \end{array} \tag{13}$$

As a result, there are three different closed states and three different open states in the channel. The two open states C_1O and C_2O connect to the two closed states C_1C_2 and C_2C_2, respectively. Two or more routes between the open states and closed states indicate that the transition matrix between open and closed states is asymmetric, and so $f_{OC}(t_O, t_C) \neq f_O(t_O) f_C(t_C)$, resulting in a memory effect of nonzero covariance between the adjacent open and closed durations. Thus a non-Markovian channel is constructed from independent Markovian subunits.

If the open state of channel is defined as only two subunits are in the open state, then there is not any correlation (data not shown). If the subunit has only one closed state and one open state, the two-subunit channel will not show any correlation no matter whether the open state of the channel is defined as at least one subunit in the open state or as both subunits in the open state (data not shown). The reason for these models giving no correlation is the zero covariance between the adjacent open and closed durations of the channel.

This discussion indicates that a nonzero covariance between the adjacent open and closed durations is a necessary condition for ACC. It requires two or more asymmetry routes between the open and closed states. Accordingly, a general model for ACC is a channel that consists of N independent subunits with each subunit having more than one closed state and at least one open state. In addition, the open state of the channel is defined as M out of N subunits in the open state with $N > M > 0$. In such a model, an asymmetry transition matrix will be defined between the open and closed time durations, resembling the situation of IP_3R channel models as discussed above.

Next, we discuss how the transition rates can affect the appearance of ACC. As displayed in Fig. 4(a), the cross correlation is calculated as a function of k_1 with $k_2 = k_1$ for different values of k_3 with $k_4 = k_3$ and $L = 1$. One can see that ACC is most evident when k_3 and k_4 are about 10 times as large as k_1 and k_2. As to the extreme situations, where k_3 and $k_4 \gg k_1$ and k_2, or k_3 and $k_4 \ll k_1$ and k_2, ACC disappears.

In addition, we consider another situation where the two subunits are not identical. We fix $k_3(1) = 1.0$ in the first

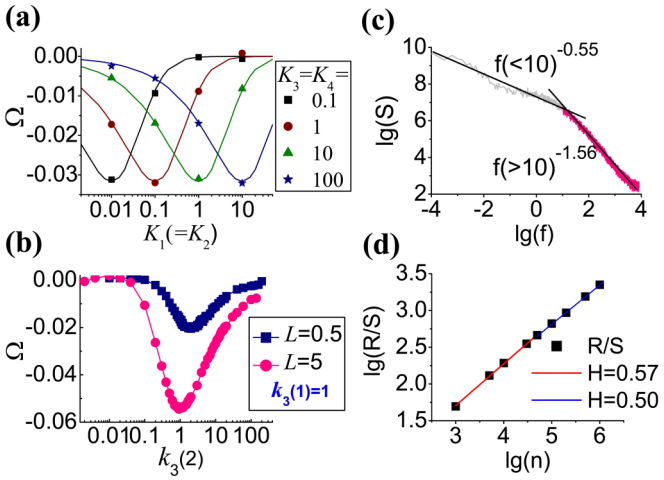

FIG. 4. (a) The cross correlation with theoretical calculations (line) and numerical simulations (symbol) as a function of $k_1(=k_2)$ with different values of $k_3 = k_4$ at $L = 1$. (b) The cross correlation via $k_3(2)$ of the second subunit of the channel with the first subunits fixed at $k_3(1) = 1.0$ with $L = 0.5$ (solid navy square) and $L = 5$ (solid pink circle). (c) The power spectra of the time series of the channel state. Linear fitting with slopes of -0.55 and -1.56 are obtained for the low-frequency range and high-frequency range, respectively. The total number of points of the time series is 1 000 000 and the interval between two data points is 0.01 s. (d) The rescaled range analysis as a function of the length n of the subseries (black solid square) with Hurst exponent obtained by a linear fitting (red solid line). The total number of points of the time series is 50 000 000 and the interval between two data points is 0.5 s. For both (c),(d), $L = 10$.

subunit and change $k_3(2)$ in the second subunit. Simulation results in Fig. 4(b) show that ACCs are found for two identical subunits at $L = 5$ and for two different subunits at $L = 0.5$. Thus, the channel with two different subunits can generate ACC also.

The ACC behavior discussed here shows a short time memory between the open (or closed) state and the following closed (or open) state in the channel. Another interesting question is if there is a long-range memory for the open and closed durations of the channel. As a result, we calculate the power spectra of the time series of the channel state [Fig. 4(c)]. Linear fitting with slopes of -0.55 and -1.56 are obtained for the low-frequency and high-frequency range, respectively. The long-term process is also discussed with the rescaled range analysis [Fig. 4(d)]. With a linear fitting, the Hurst exponent $H = 0.57$ and $H = 0.5$ are obtained for small length and large length n, respectively. These results show a persistent correlation for a short term of time series and a Wiener process for a long term of time series.

V. CONCLUSION

In summary, we show in this paper that a non-Markovian behavior, the ACC between the adjacent open and closed durations of channel, can be observed in a type of Markovian channel. In detail, a weak ACC can be found in a multimeric channel if the open state of the channel is defined as at least M out of N subunits ($N > M > 0$) are in the open state, where the subunit has at least one open state and more than one closed state. Actually by considering the detailed channel states, the transition pathways among multiple open and closed states are complex. Thus, the channel gives an asymmetry transition matrix between the open and closed states. As a result, although the subunit shows a Markovian gating dynamics between the adjacent open and closed durations, the channel can show a weak ACC between the adjacent open and closed durations, presenting a non-Markovian memory behavior.

It has been suggested that a non-Markovian time series can be generated dynamically from complex systems [5,6,9–11,13,14]. Our study indicates that there is a simple way to construct non-Markovian binary data. With several sets of binary Markovian time series generated by independent subunits, a simple sum of these time series can generate binary data with a threshold procedure. This binary time series may show a non-Markovian memory behavior of negative correlation between the adjacent open and closed durations. A general equation, i.e., Eq. (7), is given for the calculation of the cross correlation based on the matrix theory. Accordingly, a correlation can occur when the covariance between the adjacent open and closed durations is nonzero.

The weak ACC between the adjacent open and closed durations indicates a short time memory of the Markovian multimeric channel. As a confirmation, both the power spectrum and rescaled range analysis also reveal a weak correlation for short-time kinetics. However, at the long timescale there is no memory process for the open and closing dynamics of the stochastic channel.

Our simulation predicts that a weak ACC may appear for the IP_3R channel with patch clamp recording at constant Ca^{2+} concentration and IP_3 concentration. The RyR channels [40,41], large-conductance voltage-activated K^+ BK channels [42,43], and the thermosensitive transient receptor potential TRP channels [44,45] have a similar tetrameric structure as the IP_3R channel. It is not clear if these types of biological channels indeed present an ACC gating dynamics, which is an interesting question to be validated in experiment.

A further important question is what the physiological significance of ACC could be if a biological channel shows an ACC gating dynamics. It has been pointed out that different channel dynamics, including the inactivation termination mechanism or stochastic attrition, may significantly change the correlation relationships between puff or spark amplitudes, durations, rising times, and interpuff intervals [20–22]. We suggest that the weak negative correlation behavior at the single-channel level may have an effect on the correlation dynamics for puffs and sparks at the clustered channel level.

ACKNOWLEDGMENTS

We would like to thank Ian Parker for many useful conversations. We acknowledge support from the National Natural Science Foundation of China (Grants No. 11675134, No. 11874310, No. 11804114, and No. 11704318), the National Key R&D Program of China (Grant No. 2018YFD0901004), and the 111 Project (Grant No. B16029).

[1] E. Neher and B. Sakmann, Nature **260**, 799 (1976).
[2] B. Hille, *Ionic Channels of Excitable Membranes* (Sinauer Associates, Sunderland, MA, 2001).
[3] W. Gardiner, *Handbook of Stochastic Methods* (Springer, Berlin, 1990).
[4] D. Petracchi, C. Ascoli, M. Barbi, S. Chillemi, M. Pellegrini, and M. Pellegrino, J. Stat. Phys. **70**, 393 (1993).
[5] B. S. Rothberg and K. L. Magleby, J. Gen. Physiol. **111**, 751 (1998).
[6] J. A. Fernandez, R. Skryma, G. Bidaux, K. L. Magleby, C. N. Scholfield, J. G. McGeown, N. Prevarskaya, and A. V. Zholos, J. Gen. Physiol. **137**, 173 (2011).
[7] J. Timmer and S. Klein, Phys. Rev. E **55**, 3306 (1997).
[8] Z. Siwy, M. Ausloos, and K. Ivanova, Phys. Rev. E **65**, 031907 (2002).
[9] I. Goychuk and P. Hanggi, Phys. Rev. E **69**, 021104 (2004).
[10] S. M. Bezrukov and M. Winterhalter, Phys. Rev. Lett. **85**, 202 (2000).
[11] Z. Siwy and A. Fulinski, Phys. Rev. Lett. **89**, 158101 (2002).
[12] R. M. M. Smeets, U. F. Keyser, and N. H. Dekker, Proc. Natl. Acad. Sci. USA **105**, 417 (2008).
[13] M. R. Powell, I. Vlassiouk, C. Martens, and Z. S. Siwy, Phys. Rev. Lett. **103**, 248104 (2009).
[14] C. Tasserit, A. Koutsioubas, D. Lairez, G. Zalczer, and M. C. Clochard, Phys. Rev. Lett. **105**, 260602 (2010).
[15] C. Wen, S. Zeng, K. Arstila, T. Sajavaara, Y. Zhu, Z. Zhang, and S. L. Zhang, ACS Sens. **2**, 300 (2017).
[16] E. Secchi, A. Nigues, L. Jubin, A. Siria, and L. Bocquet, Phys. Rev. Lett. **116**, 154501 (2016).
[17] R. Weron, Phys. A (Amsterdam, Neth.) **312**, 285 (2002).
[18] A. Richard, P. Orio, and E. Tanre, J. Comput. Neurosci. **44**, 297 (2018).
[19] G. M. Caporale, L. Gil-Alana, and A. Plastun, J. Stat. Comput. Simul. **89**, 1763 (2019).
[20] D. Fraiman, B. Pando, S. Dargan, I. Parker, and S. P. Dawson, Biophys. J. **90**, 3897 (2006).
[21] X. Wang, Y. Hao, S. H. Weinberg, and G. D. Smith, Math. Biosci. **264**, 101 (2015).
[22] M. D. Stern, E. Rios, and V. A. Maltsev, J. Gen. Physiol. **142**, 257 (2013).
[23] M. Á Sánchez, J. E. Trinidad, J. García, and M. Fernández, PLoS ONE **10**, e0127824 (2019).
[24] J. K. Foskett, C. White, K. H. Cheung, and D. O. Mak, Physiol. Rev. **87**, 593 (2007).
[25] O. Dellis, S. G. Dedos, S. C. Tovey, Ur. R. Taufiq, S. J. Dubel, and C. W. Taylor, Science **313**, 229 (2006).
[26] I. F. Smith and I. Parker, Proc. Natl. Acad. Sci. USA **106**, 6404 (2009).
[27] G. W. De Young and J. Keizer, Proc. Natl. Acad. Sci. USA **89**, 9895 (1992).
[28] I. Bezprozvanny, J. Watras, and B. E. Ehrlich, Nature **351**, 751 (1991).
[29] R. Thul and M. Falcke, Phys. Rev. Lett. **93**, 188103 (2004).
[30] G. Ullah, D.-O. Daniel Mak, and J. E. Pearson, J. Gen. Physiol. **140**, 159 (2012).
[31] I. Siekmann, L. E. Wagner II, D. Yule, E. Crampin, and J. Sneyd, Biophys. J. **103**, 658 (2012).
[32] I. Siekmann, M. Fackrell, E. J. Crampin, and P. Taylor, Proc. R. Soc. London, Ser. A **472**, 20160122 (2016).
[33] G. Dupont and J. Sneyd, Curr. Opin. Syst. Biol. **3**, 15 (2017).
[34] B. A. Bicknell and G. J. Goodhill, Proc. Natl. Acad. Sci. USA **113**, E5288 (2016).
[35] D. O. Mak, S. McBride, and J. K. Foskett, Proc. Natl. Acad. Sci. USA **95**, 15821 (1998).
[36] J. W. Shuai and P. Jung, Phys. Rev. Lett. **95**, 114501 (2005).
[37] J. W. Shuai, J. E. Pearson, J. K. Foskett, D. O. D. Mak, and I. Parker, Biophys. J. **93**, 1151 (2007).
[38] D. Colquhoun and A. G. Hawkes, Philos. Trans. R. Soc., B **300**, 1 (1982).
[39] W. J. Bruno, J. Yang, and J. E. Pearson, Proc. Natl. Acad. Sci. USA **102**, 6326 (2005).
[40] M. Fill and J. A. Copello, Physiol. Rev. **82**, 893 (2002).
[41] W. Peng, H. Shen, J. Wu, W. Guo, X. Pan, R. Wang, S. R. Wayne, and N. Yan, Science **354**, aah5324 (2016).
[42] B. S. Rothberg and K. L. Magleby, J. Gen. Physiol. **116**, 75 (2000).
[43] R. Latorre, K. Castillo, W. Carrasquel-Ursulaez, R. V. Sepulveda, F. Gonzalez-Nilo, C. Gonzalez, and O. Alvarez, Physiol. Rev. **97**, 39 (2017).
[44] I. Diaz-Franulic, H. Poblete, G. Mino-Galaz, C. Gonzalez, and R. Latorre, Annu. Rev. Biophys. **45**, 371 (2016).
[45] F. Yang and J. Zheng, Protein Cell **8**, 169 (2017).